Journal of Computational Methods in Sciences and Engineering 10 (2010) 1–20 1
DOI 10.3233/JCM-2010-0326
IOS Press

Molecular dynamics calculation of infra-red spectra of ultra-dispersed atmospheric moisture

A.Y. Galashev
Institute of Industrial Ecology, Ural Division, Russian Academy of Sciences, Sofia Kovalevskaya Str., 20a, Yekaterinburg, 620219 Russia

Abstract. The absorption and scattering of IR radiation by aqueous ultradisperse systems that absorb nitrogen, oxygen, or argon are studied with the molecular dynamics method on the basis of a flexible molecule model. After nitrogen or argon is captured by an aqueous disperse system, the absorption of the IR radiation by this system increases owing to the enhancement of intramolecular vibrations. It is demonstrated that the integral intensity of absorption of IR radiation decays after water clusters adsorb oxygen. As the nitrogen concentration in a system of water clusters rises, the power of IR radiation emitted by the system increases significantly. The attachment of molecular oxygen by clusters leads to decay of the power of their IR radiation, while the capture of atomic oxygen, on the contrary, is accompanied by an increase in the rate of dissipation of energy accumulated by water aggregates. The power of radiation generated by cluster systems at the expense of thermal energy increases considerably when there is one adsorbed argon atom per cluster and decreases with a twofold increase in the number of argon atoms in clusters.

Keywords: Absorption, infra-red spectra, argon, nitrogen, oxygen, power of radiation, water clusters

1. Introduction

The analysis of the evolution of the chemical composition of Earth's atmosphere indicates that, two billion years ago, it consisted by 96% of molecular nitrogen [1]. Later, the composition of atmosphere has begun to change toward an increase in the content of molecular oxygen. At present, the composition of Earth's atmosphere does not comply with the content of various elements in the cosmic substance. Current Earth's atmosphere composed by 78.084 vol % of nitrogen, 20.946% of oxygen, 0.932% of argon and 0.038% of others gases. Nitrogen is the most representative component of a troposphere where the main mass of water vapor is also accumulated. Molecular nitrogen is soluble in water and, hence, can be captured by small water formations (clusters) that finally grow to the droplet size. Nitrogen atoms are capable of forming H-N-H groups, that is, hydrogen bonds, in the environment of water molecules [2]. The gas dissolved in water droplets always tends to come in equilibrium with the gas in the atmosphere. Nitrogen in the amount of more than 0.01 Gt per year falls onto the Earth with the atmospheric precipitation. This gas only indirectly affects the transfer of thermal radiation. Nitrogen is not among the main absorbing and radiating components of Earth's atmosphere (e.g., H_2O and CO_2);

*Corresponding author. Tel.: +7 343 3623267; Faz: +7 343 3743771; E-mail: galashev@ecko.uran.ru.

however, it noticeably affects the radiation transfer in atmospheric transparency windows for water vapor and carbon dioxide.

The flux of ultraviolet (UV) solar radiation, which carries about 1% of the incoming solar energy, comes to altitudes of 20–40 km, where it is absorbed by ozone to cause its dissociation. However, a large fraction of energy of UV radiation dissipates at altitudes of 80–100 km and causes dissociation of molecular oxygen. Above 100 km, hard UV radiation performs the primary ionization of the atmosphere, as well as its heating. In this region, the temperature increases with altitude, and its variation is defined both by heating due to UV radiation and by heat removal downwards by molecular and turbulent thermal conductivity.

One of the natural sources of oxygen may be provided by water. The effect of UV radiation on water results in the generation of atomic and molecular oxygen and hydrogen in the upper atmosphere of the Earth (above the ozone layer). Lighter-than-air hydrogen escapes from the terrestrial atmosphere, and oxygen, on the contrary, stays there [3]. In general, the properties of natural water largely depend on oxygen it contains. The presence of calcite, magnesium, and other solutes in water leads to the binding of a part of oxygen. The concentrations of these substances may be most different; therefore, one must expect an even greater diversity of properties in the case of water saturated with oxygen. Dissolved oxygen and calcite make water a magnetic medium [4]. The observed paramagnetism is largely due to the presence of uncompensated magnetic moments which arise because of oxygen. As a rule, the nature of these moments is associated with the orbital motion of electrons, their spin.

The abundance of argon on Earth is greater than all other elements of its group. In water, argon is dissolved better than nitrogen. Argon atoms have no dipole moments. By the calculation of the surface of pair-additive potential energy, it was shown that the most advantageous structure of argon atoms captured one water molecule is the icosahedron containing H_2O molecule in its center [5]. Quantum-chemical calculations indicate that, upon the capture of argon atoms by grouping water molecules, pentagonal dodecahedron composed of water molecules and containing argon atom in its interior is formed with higher probability [6]. The presence of argon atoms in a water cluster should lead to changes in vibration frequencies of water molecules and their intramolecular vibrations that is reflected in the IR spectra. The effect of absorption of atmospheric gases on the spectral characteristics of water clusters has not so far been studied.

Water vapor in atmosphere plays a key role for the energy budget of our planet. The so-called water vapor continuum absorption was explained by the suggestion that hydrogen bonded water dimers could contribute to the continuum [7]. Besides water dimers are also postulated to catalyze the formation of atmospheric H_2SO_4. Really ab initio calculations and experimental results have confirmed this hypothesis [8–11]. The abundance of water dimers in the atmosphere may be important for modeling water recondensation [12]. It was predicted that radical complexes like $HO_2 \cdot H_2O$ exist in relatively high concentrations in the atmosphere [13,14]. In work [15] both experimental and theoretical support was given for the existence of electrically neutral clusters in the atmosphere. According to this work the concentration of clusters can reach the value of $2{\cdot}10^5$ cm^{-3} at supercooling of about 46 K. Water clusters could form aerosols or catalyze into acid rain in the atmosphere. Water clusters might also be involved in a variety of chemical processes in the atmosphere. The results of work [16] using the most accurate water pair potential [17] indicate that water dimers can exist in sufficient concentrations (e.g., 10^{16} cm^{-3} at 313 K and 100% relative humidity) to affect physical and chemical processes in the atmosphere. For accuracy of dimer calculation it is very important to calculate the concentration of other water clusters in the troposphere. The refraction index of water clusters only slightly depends on the intensity of the external electromagnetic field. Therefore as investigated in other works [18,19]

the phenomenon of light wave concentration is not observed in this medium, that is, self-focusing of the light does not occur. Autoregulation of the atmospheric composition due to the formation of water clusters and their subsequent capture of the most abundant atmospheric gases (nitrogen, oxygen, argon) are, as a rule, ignored in the estimation of the Earth's radiation balance.

The aim of this work is to study the absorption of molecular nitrogen and oxygen as well as atoms of oxygen and argon by water clusters and to determine the effect of their absorption by aqueous disperse medium on the IR absorption spectra. In our research we use the molecular dynamics (MD) method and flexible molecule model.

2. Model

The account of the polarizability in the model makes it possible to investigate nonuniform and isotropic properties of water, for example, near the surface separating the liquid from the solid body or gas. When studying the behavior of water molecules near the molecules of another kind, the important role is assigned to the degrees of freedom that are responsible for the fast response of electron subsystem. It could be expected that, upon the interaction with water clusters, atoms and molecules of impurities tend to penetrate inside the polar medium. However, their motion to the depth of water cluster is related with the large work done on the rearrangement of cluster structure. In this case, the hydrophobic effect is manifested that hampers the construction of the cell from water molecules around the impurity but stabilizes such cell in the bulk water.

The use of intramolecular flexibility allows us to more precisely describe some vibrational properties of water molecules and their deformation at perturbations. Many of these effects are related with the influence of molecules of another kind or the presence of interfaces. However, substantial changes in the dipole moments of molecules and, hence, in dielectric properties of molecules under the action of temperature and pressure can also occur in pure water. The account of intramolecular flexibility and electronic polarizability in the model enables us to better understand changes in some special properties of water, but, in general, this does not improve the accuracy of determining its thermodynamrc and structural characteristics, as compared with traditional models of rigid molecules. In particular, there is no improvement in describing the maximum of density of water and its thermodynamrc properties at high temperatures [20]. However, the use of the flexible molecule model leads to more accurate calculation of spectra of reflection of IR radiation by aqueous disperse media [21]. This study is based on the construction of flexible molecule model by the procedure developed in [22–24]. The calculation of spectral characteristics in such model was performed in [25]. Here, we used analogous procedure for this purpose.

In this work, water-water interactions are considered on the basis of the modified TIP4P model of water [26]. The total interaction energy of the water system can be written as

$$U_{tot} = U_{pair} + U_{pol}, \tag{1}$$

where the pairwise additive part of the potential is the sum of the Lennard-Jones (LJ) and Coulomb interactions,

$$U_{pair} = \sum_i \sum_j \left(4\varepsilon_{LJ} \left[\left(\frac{\sigma_{ij}}{r_{ij}} \right)^{12} - \left(\frac{\sigma_{ij}}{r_{ij}} \right)^{6} \right] + \frac{Q_i Q_j}{r_{ij}} \right). \tag{2}$$

Table 1
Potential parameters for water-water interactions used in the MD simulation. σ_{ij} and ε_{LJ} are the Lennard-Jones parameters, Q_i is atomic charge, and α^p is the molecular polarizability

Atom type	σ_{ij} (nm)	ε_{LJ} (kJ/mol)	Q_i (e)	α^p (Ï^3)
O	0.3234	0.7634	–	–
H	–	–	0.5190	–
A	–	–	-1.0380	1.49

Table 2
Potential parameters of nitrogen-nitrogen and nitrogen-water interactions

Atom type	σ_{ij} (nm)	ε_{LJ} (kJ/mol)	Q_i (e)	α^p (Ï^3)
N-N	0.3310	1.2968	-0.4954	2.43
N-O(A)	0.3282	2.1125	-0.4954, -1.0380	2.43, 1.49
N-H	–	–	-0.4954, 0.5190	–

Table 3
Potential parameters of oxygen-oxygen and oxygen-water interactions

Atom type	a_i (kJ/mol Ï^6)	b_i (kJ/mol)	c_i (nm^{-1})	α^p (Ï^3)
O-O(A)	31.921	504.030	18.990	1.57, 1.49
O-H	24.855	176.119	15.965	–

Here, Q_i are the charges localized on interacting centers and r_{ij} are distances between the centers; parameters ε_{LJ} and σ_{ij} of potential describing these interactions are tabulated in Table 1. The water molecule geometry is represented using experimental gas phase O $-$ H bond lengths of 0.09572 nm and a H-O $-$ H bond angle of 104.5° [27]. Fixed charges are assigned to H atoms and at a point (A) on bisector of the H-O $-$ H angle that is 0.0215 nm away from the oxygen atom.

The additive part of nitrogen-nitrogen and nitrogen-water interactions is set by the sum of Lennard-Jones and Coulomb contributions:

$$\Phi(r_{ij}) = 4\varepsilon_{LJ}\left[\left(\frac{\sigma_{ij}}{r_{ij}}\right)^{12} - \left(\frac{\sigma_{ij}}{r_{ij}}\right)^{6}\right] + Q_iQ_j/r_{ij}, \tag{3}$$

potential parameters are taken from [26,28] and given in Table 2. LJ parameters were established with the use of the second virial coefficients. Numerical estimations of the second virial coefficients are made for gases N_2 and O_2 by S. Kielich [29].

The dynamics of system of the water and oxygen molecules were realized with description of oxygen-oxygen and oxygen-water interaction in the form of the sum of repulsion and dispersion contributions [30],

$$\Phi(r_{ij}) = b_ib_j\exp[-(c_i+c_j)r_{ij}] - a_ia_jr_{ij}^{-6}, \tag{4}$$

where the parameters a_i, b_i, and c_i of the potential describing these interactions were borrowed from [31] and are shown in Table 3.

Argon-water pair potential obtained by ab initio calculations can be presented in the form [32]

$$\Phi(r) = \frac{\varepsilon_m}{\beta-6}\left[6\exp\left[\beta\left(1-\frac{r_{ij}}{r_m}\right)\right] - \left(\frac{r_{ij}}{r_m}\right)^{6}\right], \tag{5}$$

Table 4
Parameters of atom-atom interaction potential of $Ar - H_2O$ system

Systems	Exponent 6			Repulsion	α^p (Å^3)
	ε_m/k (K)	r_m (nm)	β	B (nm^{12}kJ/mol)	
$Ar - OH_2(A)$	156.8	0.3556	12.5	–	1.66, 1.49
$Ar - HOH$	–	–	–	$5.2667 \cdot 10^{-7}$	–

where r_{ij} is the distance between argon and oxygen atoms. The values of potential parameters ε_m, β, r_m are listed in Table 4. However, the calculation of interaction energy between water molecules and argon atom leads to some discrepancy between the results obtained using formula (5) and by direct ab initio calculations. The delocalization of electrons along the hydrogen bond creates the effect of additional force acting on atom (molecule) occupying the guest cell. In order to account for the effect of the hydrogen bond in the argon-water system, pair atom-atom potential (5) should be corrected for the changes in $Ar - H \cdot OH$ interaction. Additional $Ar - H \cdot OH$ interaction was taken into account by the inclusion of interaction potential characterizing pure repulsion [33]

$$\Phi_{repul}(r) = \frac{B}{r_{ij}^{12}}. \tag{6}$$

The value of parameter B is given in Table 4. The use of additional interaction potential in the form of Eq. (6) makes it possible to minimize the errors in describing the interaction between guest argon atom and water molecules creating the cell for this atom. Very weak argon-argon interaction was calculated with use of the Lennard-Jones potential. Interatomic distances in the N_2 and O_2 molecules are $r_{\mathrm{NN}} = 0.1094$ nm and $r_{\mathrm{OO}} = 0.12074$ nm correspondingly [34].

The nonadditive part of interaction was represented by the polarization contribution. The averaged polarizabilities of the N_2, O_2 molecules, and Aratoms ($\alpha^p = 2.43$, 1.57, and 1.66 Å^3) were referred to its center of mass. Polarization energy is defined by the relation

$$U_{pol} = -\frac{1}{2}\sum_i \mathbf{d}_i \mathbf{E}_i^0, \tag{7}$$

where, $\mathbf{E}_i^0$, is the strength of electric field in point i induced in a system by fixed charges

$$\mathbf{E}_i^0 = \sum_{j \neq i} \frac{Q_j \mathbf{r}_{ij}}{r_{ij}^3}, \tag{8}$$

$\mathbf{d}_i$, is the induced dipole moment of the ith atom

$$\mathbf{d}_i = \alpha_i^p \mathbf{E}_i, \tag{9}$$

where

$$\mathbf{E}_i = \mathbf{E}_i^0 + \sum_{j \neq i} \mathbf{T}_{ij} \cdot \mathbf{d}_j, \tag{10}$$

Here, $\mathbf{E}_i$, is the strength of the total electric field in the center of ith atom and $\mathbf{T}_{ij}$ is the dipole tensor

$$\mathbf{T}_{ij} = \frac{1}{r_{ij}^3}\left(\frac{3\mathbf{r}_{ij}\mathbf{r}_{ij}}{r_{ij}^2} - 1\right), \tag{11}$$

To calculate induced dipole moments at each time step, we used standard iterative procedure [26]. The accuracy of determining $\mathbf{d}_i$, was set within the $10^{-5} \div 10^{-4}D$ range.

Flexible molecule models were described within the framework of the Hamiltonian dynamics in [22, 23]. Let a and b atoms be separated in a diatomic molecule by the distance:

$$q = \|\mathbf{r}_a - \mathbf{r}_b\|, \tag{12}$$

where $\mathbf{r}_a$ and $\mathbf{r}_b$ are the vectors determining positions of atoms. We denote corresponding velocities by $\mathbf{v}_a$ and $\mathbf{v}_b$ and the reduced mass is defined as

$$\mu = \frac{m_a m_b}{m_a + m_b}. \tag{13}$$

The size of a molecule represented by a and b atoms is determined from the condition of the equality of total potential force, $\mathbf{f}(\mathbf{q}) = -\frac{\partial \mathbf{r}}{\partial \mathbf{q}} \nabla \Phi(\mathbf{r})$ and centrifugal $-\mu q \omega^2$

$$-\mu q \omega^2 - \mathbf{f}(\mathbf{r}) \frac{\partial \mathbf{r}}{\partial \mathbf{q}} = 0, \tag{14}$$

where $\omega = \|\mathbf{v}_a - \mathbf{v}_b\| / q$ is the angular velocity. From the condition of the minimum of the contribution from each generalized coordinate to potential energy U, we obtain

$$\frac{\partial}{\partial q_i} H(\mathbf{r}, \mathbf{v}) = \frac{\partial}{\partial q_i} \left(\frac{1}{2} \mu_i q_i^2 \omega_i^2 + U(\mathbf{r}) \right) = 0. \tag{15}$$

This method is generalized to the molecules of any composition [24].

The study of the adsorption of impurity by water clusters began with the construction of the configuration composed of an equilibrium water cluster and surrounding molecules or atoms of impurity. Initial equilibrium configurations of water clusters were obtained in separate molecular dynamics calculations. In this case, the kinetic energy of molecules constituting cluster corresponded to the temperature of 233 K. Initially, the center of the mass of impurity molecules (one or two) was placed at a distance of 0.6–0.7 nm from the nearest atom of the water cluster so that each atom of the impurity molecule fell in the field of molecular interaction. The cut-off radius of all interactions in the model was equal to 0.9 nm. A linear N_2 or O_2 molecule was oriented along the ray connecting its center with the center of cluster mass. When two molecules and two or four atoms were added to the cluster, with each pair arranged along the same ray, but on opposite sides of the cluster. A newly formed system was equilibrated within a time interval of $0.6 \times 10^6 \Delta t$, where the time step $\Delta t = 10^{-17}$s; then, necessary physicochemical properties were calculated within an interval of $3 \times 10^6 \Delta t$ The equations of the motion of the centers of mass of the molecules were integrated by the Gear fourth-order method [35]. The equations of rotational motion for the angular coordinates of the molecules were analytically solved using the Rodrigues-Hamilton parameters [36,37]. The integration scheme for equations of motion involving rotations corresponded to the approach proposed by Sonnenschein [38]. Thermodynamic properties of water clusters and their structure depend on the model employed. For example, for $(H_2O)_{20}$ cluster, the difference in the energy of most favorable structures of POL1 [39] and SPC/E [40] models is equal to 13.4%. In our model, the energy of $(H_2O)_{20}$ cluster at $T = 233$ K is intermediate between corresponding energies for POL1 and SPC/E models and is determined as -8.66 eV.

3. Dielectric properties

If the mean free path l of a molecule is much shorter than wavelength λ, the coefficient of extinction (attenuation) h of the incident beam is determined, on the one hand, by the Rayleigh formula [41], and on the other hand, through the scattering coefficient ρ ($h = \frac{16\pi}{3}\rho$) [42]. Taking into account that $h = \alpha + \rho$, where α is the absorption coefficient, we have

$$N = \frac{2\omega^4}{3\pi c^4}\frac{(\sqrt{\varepsilon}-1)^2}{\alpha}(1-\frac{3}{16\pi}), \tag{16}$$

where N is the number of scattering centers in 1 cm^3. Here, c is the speed of light, ε is the dielectric permittivity of a medium, and ω is the frequency of the incident wave.

Let us classify ultradisperse systems using statistical weights for constituting clusters. The following systems were generated: I –$(H_2O)_i$, II – $N_2(H_2O)_i$, III – $(N_2)_2(H_2O)_i$, IV – $O_2(H_2O)_i$, V – $(O_2)_2(H_2O)_i$, VI – $(O)_2(H_2O)_i$, VII – $(O)_4(H_2O)_i$, VIII – $Ar(H_2O)_i$, IX – $(Ar)_2(H_2O)_i$, $10 \leqslant i \leqslant 50$, step $\Delta i = 5$. Let us form II-IX systems so that the cluster containing j molecules (atoms) of impurity and i molecules of water has a statistical weight of

$$W_{ji} = \frac{N_{ji}}{N_\Sigma}, j = 1, 2, \ldots, i = 10, 15, \ldots, 50, \tag{17}$$

where, N_{ji} is the number of clusters containing j molecules (atoms) of impurity and i molecules of water in 1 cm^3 and $N_\Sigma = \sum_{k=1}^{9} N_k$; k characterizes the set of subscripts i and j. For example, at $k = 1$, the i value is always equal to 10 and the j values can be 1 or 2. Analogous weights were used for $(H_2O)_i$, clusters forming system I. Hereafter, all spectral characteristics were calculated with the account of accepted statistical weights W_{ji}. Static dielectric constant ε_0 was calculated through the fluctuations of total dipole moment $\mathbf{M}$ [43]

$$\varepsilon_0 = 1 + \frac{4\pi}{3VkT}\left[\langle \mathbf{M}^2\rangle - \langle \mathbf{M}\rangle^2\right]. \tag{18}$$

Dielectric permittivity $\varepsilon(\omega)$ was represented by the complex value $\varepsilon(\omega) = \varepsilon'(\omega) - i\varepsilon''(\omega)$, which was calculated using the following equation [44,45]:

$$\frac{\varepsilon(\omega)-1}{\varepsilon_0-1} = -\int_0^\infty \exp(-i\omega t)\frac{dF}{dt}dt = 1 - i\omega\int_0^\infty \exp(-i\omega t)F(t)dt, \tag{19}$$

where the $F(t)$ function represented the normalized autocorrelation function of the total dipole moment of a cluster

$$F(t) = \frac{\langle \mathbf{M}(t)\cdot\mathbf{M}(0)\rangle}{\langle \mathbf{M}^2\rangle}, \tag{20}$$

The real part of ε' has the physical meaning of relative dielectric permittivity, while the imaginary part of ε'' characterizes the losses and is called the dielectric loss factor.

The absorption coefficient of outer IR radiation,α, can be represented through the imaginary part of frequency-dependent dielectric permittivity $\varepsilon(\omega)$ in the form [44]

$$\alpha(\omega) = 2\frac{\omega}{c}Im[\varepsilon(\omega)^{1/2}]. \tag{21}$$

Frequency dispersion of dielectric permittivity defines the frequency dependence of dielectric losses $P(\omega)$ in accordance with the expression [42]

$$P = \frac{\varepsilon'' < E^2 > \omega}{4\pi}, \tag{22}$$

where $< E^2 >$ is the average value of the squared strength of electric field and ω is the frequency of emitted electromagnetic wave.

4. Calculation results

4.1. Nitrogen

In the molecular dynamics investigation of gas hydrates containing O_2 and N_2 guest molecules, no significant differences in the behavior of these molecules were revealed within the cell occupied by the molecules [46]. Therefore, it was of interest to compare the configurations of $(O_2)_2(H_2O)_{50}$ and $(N_2)_2(H_2O)_{50}$ clusters prepared by the addition (to the same water cluster) of different molecules (O_2 and N_2) with the identical positions of the centers of mass at the initial moment and orientations with respect to water cluster. The coefficient of absorption of gas by water presents the volume of gas (measured at $T = 273$ K), which is dissolved in a solvent unit volume at the gas partial pressure equals 1 MPa. For oxygen (0.491), this coefficient more than twofold exceeds the value for nitrogen (0.236) [47]. At the time of 30 ps, the oxygen molecule is oriented tangentially with respect to the cluster surface, whereas the orientation of N_2 molecules is most likely arbitrary. The orientation of oxygen molecules is set by the hydrogen atoms of surface water molecules that are usually oriented outward the cluster. The interaction between N_2 molecules and hydrogen atoms is more "rigid" and the repulsion branch of interaction potential is steeper in this case than at the O-H interaction. The lower (in Fig. 1) N2 molecule is situated at longer distance from the cluster than corresponding O_2 molecule. For example, at the absorption of nitrogen by water cluster, its lower solubility in water is exhibited.

The values of the real part of dielectric permittivity ε' of the system of pure water clusters (system I) at frequencies $0 \leqslant \omega \leqslant 2500$ cm^{-1} markedly exceed the corresponding values for systems II and III of clusters containing nitrogen (Fig. 2). In this frequency range, the $\varepsilon'(\omega)$ function of system I has two maxima fitting frequencies 805 and 1220 cm^{-1}. This function is characterized by the third maximum in the vicinity of 3417 cm^{-1}. In a frequency range $2520 \leqslant \omega \leqslant 3110$ cm^{-1}, the values of ε' for systems II and III can be slightly higher than for system I. Major maxima of the $\varepsilon'(\omega)$ function for systems II and III fall on frequencies 2740 and 3404 cm^{-1}, respectively. The $\varepsilon'(\omega)$ function for bulk water in the TIP4P model [48] (Fig. 2a, curve 4) rapidly decays with the frequency and already at $\omega > 60$ cm^{-1} has lower values than analogous functions for considered disperse systems. In the $130 \leqslant \omega \leqslant 1800$ cm^{-1} frequency range, the values of the imaginary part of dielectric permittivity for system I exceed the analogous values for systems II and III (Fig. 2b) and, at frequencies $\omega > 1870$ cm^{-1}, are lower than corresponding characteristics for systems II and III. Electric losses always present in real substance in a variable electromagnetic field, therefore $\varepsilon'' \neq 0$, if $\omega \neq 0$. As frequency grows values of $\varepsilon''(\omega)$ functions in the disperse water medium enriched with nitrogen, increase. Major maxima of the$\varepsilon''(\omega)$ function for systems I, II, and III are localized at 702, 2867, and 3187 cm^{-1}, respectively. In the $\omega > 690$ cm^{-1} range, experimental values of ε'' for bulk water [49] (Fig. 2b, curve 4) become smaller than the ε'' value for each of considered disperse systems.

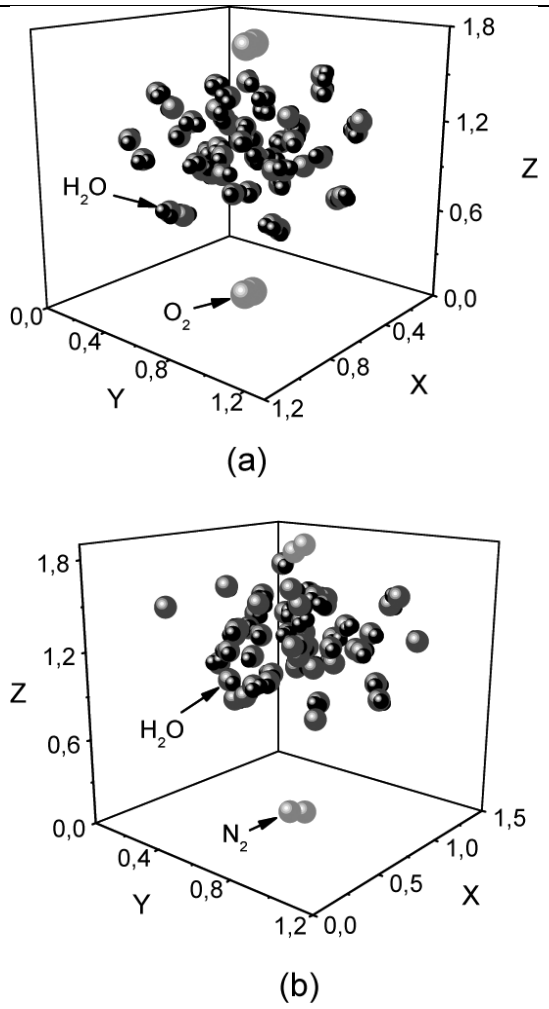

Fig. 1. Configurations of (a) $(O_2)_2(H_2O)_{50}$ and (b) $(N_2)_2(H_2O)_{50}$ clusters corresponding to time of 30 ps. Coordinates of molecules are presented in nanometers.

In the range of lower frequencies ($\omega < 1000$ cm^{-1}), the intensities of the absorption (coefficient α) of IR radiation of disperse systems I-III differ slightly (Fig. 3). However, at $\omega > 1300$ cm^{-1}, stronger absorption of nitrogen-containing disperse systems is observed, as compared with the system of pure water clusters. Moreover, the intensity of IR radiation decreases with an increase in the nitrogen concentration in the disperse system. The localization of the major maximum of the $\alpha(\omega)$ function is not changed after the capture of nitrogen molecules by water clusters and corresponds to the frequency of 3187 cm^{-1} for each considered disperse systems I-III. The $\alpha(\omega)$ spectrum of bulk water (Fig. 3, curve 4) is characterized by five maxima at frequencies of 200, 700, 1643, 2127, and 3407 cm^{-1} [50]. The origin of the first maximum is explained by translational vibrations including the contributions by stretching (compression) and buckling of hydrogen bonds [51]. The second peak is most likely associated with librations of molecules existing because of limitations due to neighboring hydrogen bonds [52]. The third peak is largely due to deformation vibrations of molecules, and the fourth peak – to the interaction of deformation vibrations and librations. Extreme points of disperse systems I-III, the nearest to the

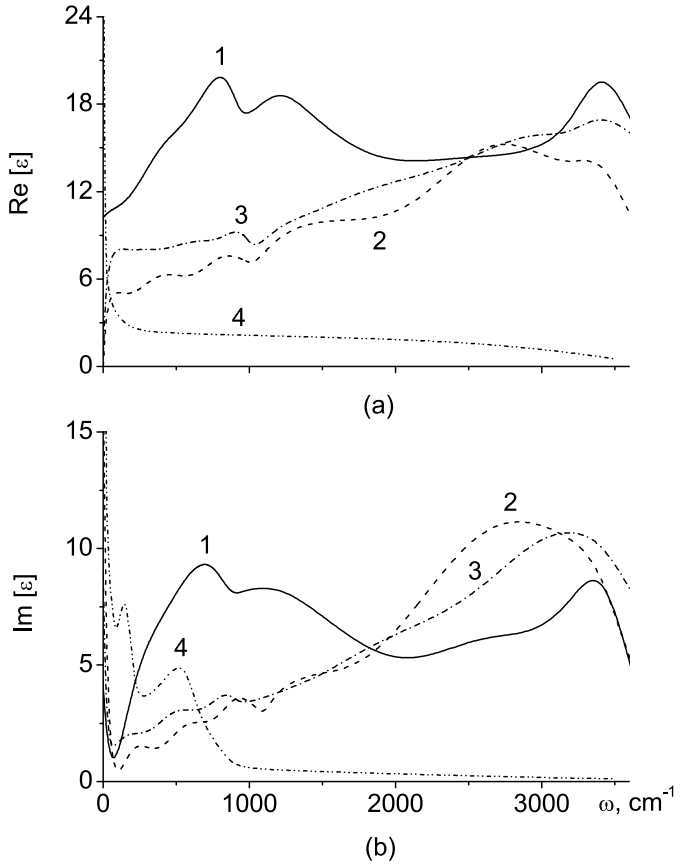

Fig. 2. Frequency dependences of (a) real and (b) imaginary parts of dielectric permittivity for disperse systems (1) I, (2) II, and (3) III, and (4) bulk water. Panel (a): calculation, TIP4P model [48]. Panel (b): experiment [49].

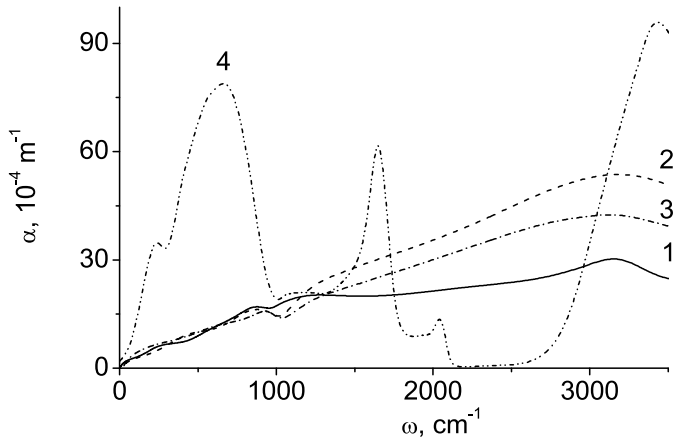

Fig. 3. The coefficient of absorption of IR radiation by the systems of molecular clusters: (1) system I, (2) system II, (3) system III, and (4) bulk water, experiment [49].

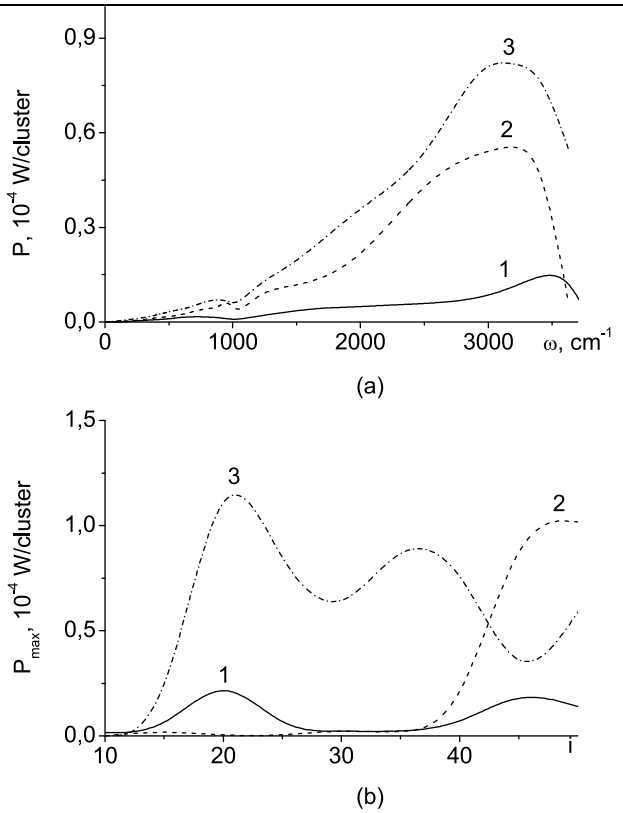

Fig. 4. Panel (a): the power of IR radiation generated by cluster systems (1) I, (2) II, and (3) III. Panel (b): dependences of the maximal values of dielectric losses on the number of water molecules in (1) $(H_2O)_i$, (2) $N_2(H_2O)_i$N2(H2O) and (3) $(N_2)_2(H_2O)_i$ clusters.

position of the second maximum of $\alpha(\omega)$ function for bulk water, refer to frequencies 702, 850, and 910 cm^{-1}, respectively. The values of this frequency for systems II and III are not strictly defined by frequencies of basic phonons of aqueous system I and can vary due to inharmoniousness [53].

Clusters absorbing the energy of IR radiation reemit this energy. The rate of energy dissipation increases abruptly when clusters capture nitrogen molecules (Fig. 4a), the radiation power being increased with the nitrogen concentration in aqueous disperse system. Maxima of energy reemission fall on frequencies 3440, 3190, and 2970 cm^{-1} for systems I, II, and III, respectively. Maximum rates of the scattering of the stored energy for these systems are rated as 1: 3.7: 5.5. Maximum radiation powers $P_{\max}$ characterizing separate cluster of systems I-III are shown in Fig. 4b. Of pure water clusters, the highest power of thermal radiation is exhibited by $(H_2O)_{20}$ and $(H_2O)_{45}$ clusters. It is seen that the largest $P_{\max}$ values for dispersed water-nitrogen systems refer to $N_2(H_2O)_{50}$, and $(N_2)_2(H_2O)_{20}$ clusters. The addition of one N_2 molecule does not perceptibly increase the $P_{\max}$ value until the size of water cluster achieves the magnitude of $i = 40$.

4.2. Oxigen

The molecules or atoms of oxygen were initially located at such a distance from $(H_2O)_n$ clusters that the interatomic spacings r_{OO} and r_{OH} between molecules of different sorts were at least 0.6 nm.

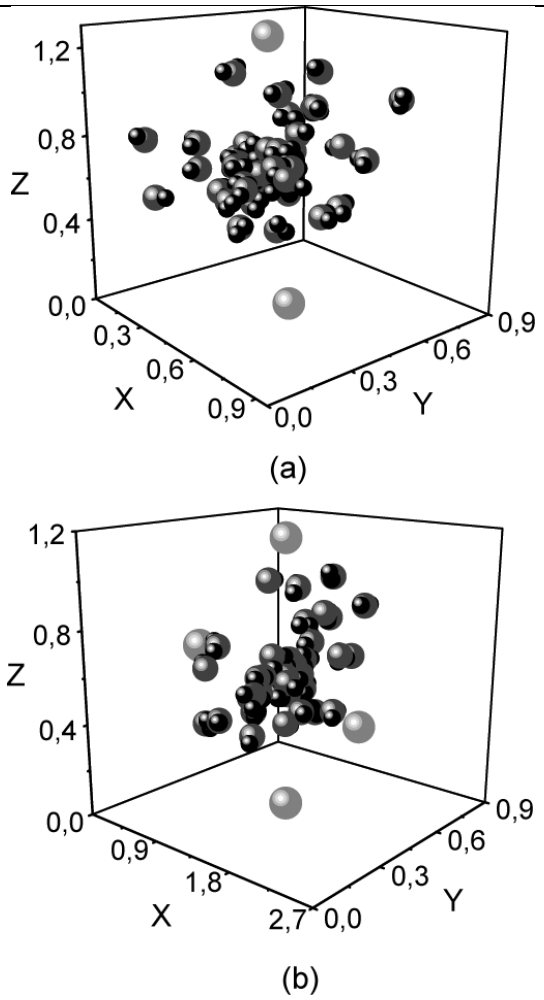

Fig. 5. Configurations of (a) $(O)_2(H_2O)_{40}$ and (b) $(O)_4(H_2O)_{40}$ clusters corresponding to time of 30 ps.

Therefore, an O_2 molecule or an O atom, which experienced attraction, moved away from their initial position toward a water cluster and either stopped, and were then held at some distance from the cluster, or deposited directly on the cluster surface. The configuration of a water cluster, which consisted of 40 molecules and adsorbed two O atoms, is given in Fig. 5a; the configuration of a similar cluster with four attached oxygen atoms is given in Fig. 5b. Adsorbed O atoms partly attract some water molecules from the cluster; in so doing, the cluster retains its integrity. However, atoms are encountered, which behave rather passively and neither are attracted to the surface nor move far away from the cluster. This is the manifestation of limited solubility of atomic oxygen in dispersed water medium.

Frequency dependences of the real and imaginary part of dielectric permittivity of water disperse systems are given in fig. 6. Absorption of both atomic and molecular oxygen by disperse systems results in reduction of values of dielectric permittivity (both real, and imaginary components) in all a investigated frequency range. And values ε' and ε'' the below, than above O or O_2 concentration in disperse water systems. We shall notice, that as against pure disperse water (curve 1) ε' and ε'' values for the systems enriched with oxygen, in a range from 1000 up to 2500 cm^{-1} not strongly change with frequency. A

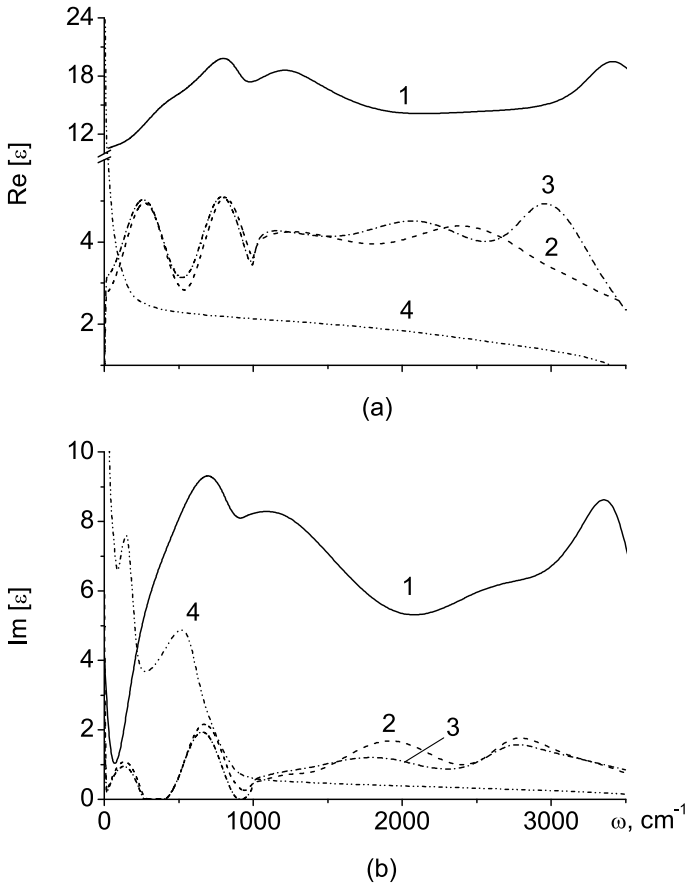

Fig. 6. (a) Real and (b) imaginary parts of the dielectric permittivity of disperse systems (1) I, (2), IV, and (3) V, and (4) bulk water. Panel (a): calculation, TIP4P model [48]. Panel (b): experiment [49].

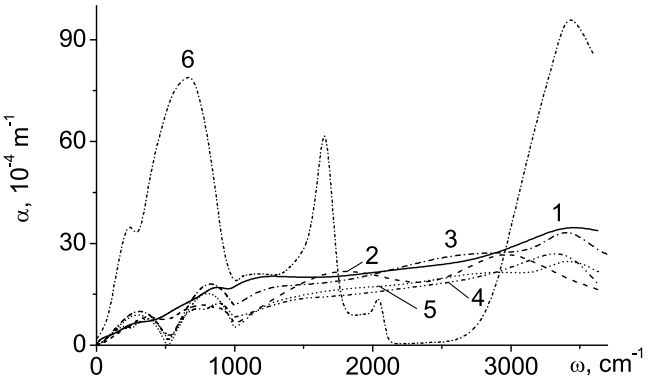

Fig. 7. The coefficient of absorption of IR radiation by systems of clusters: (1) system I, (2) IV, (3) V, (4) VI, (5) VII, (6) liquid water, experiment [50].

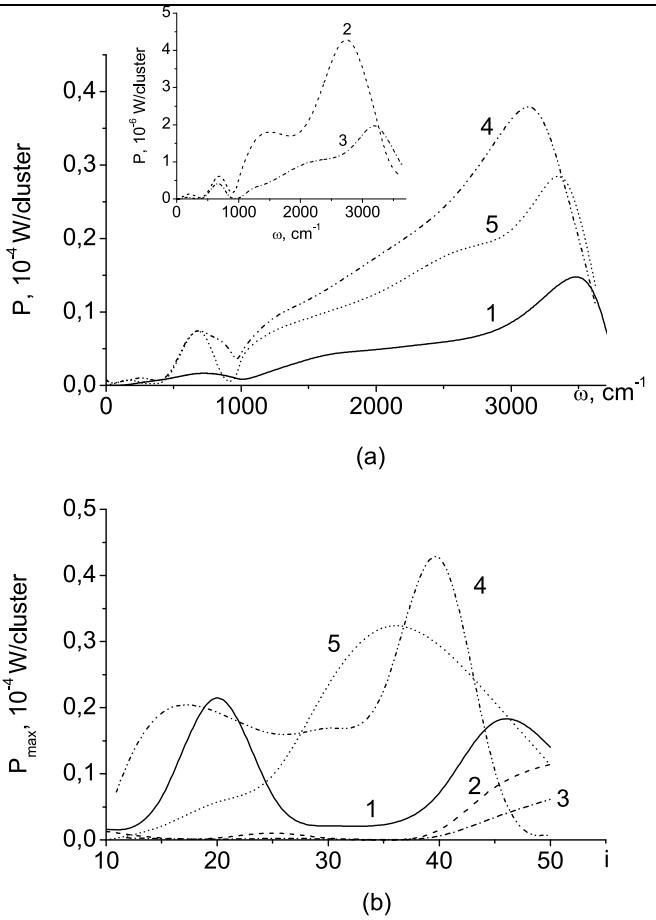

Fig. 8. (a) The power of scattering of IR radiation by systems of clusters: (1) system I, (2) IV, (3) V, (4) VI, (5) VII; and (b) the maximal rate of scattering of energy as a function of the number of water molecules i in clusters: (1) $(H_2O)_i$, (2) $O_2(H_2O)_i$, (3) $(O_2)_2(H_2O)_i$, (4) $(O)_2(H_2O)_i$, (5) $(O)_4(H_2O)_i$.

twofold increase in the concentration both atomic, and molecular oxygen results in reduction of values ε' and ε''.

The absorption coefficient α of IR radiation for disperse systems increases with frequency (Fig. 7). The $\alpha(\omega)$ spectra of disperse systems I, IV–VII have several maxima and minima. The strongest increase in the coefficient a of pure disperse water occurs in the frequency range from zero to 1000 cm^{-1}. For system IV, the first two peaks at $\omega < 1000$ cm^{-1} turn out to be weakly separated; however, for systems V-VII, they are already quite well resolved. In the absence of dissociation of oxygen captured by disperse systems, the values of the functions $\alpha(\omega)$ ascribed to these systems in the range $0 \leqslant \omega \leqslant 3500$ cm^{-1} periodically become higher or lower than the respective values for pure disperse water. The integral intensities of absorption of IR radiation by systems I, IV–VII correlate as 1: 0.56: 0.50: 0.68: 0.54. A twofold increase in the concentration of molecular and atomic oxygen in water clusters gives an 9.3% and 19.6% decrease in integral IR absorption respectively. The principal maximum of the function $\alpha(\omega)$ for systems IV–VII is in the frequency range $3200 \leqslant \omega \leqslant 3410$ cm^{-1}. Curve 6 in Fig. 7 indicates the experimentally obtained IR radiation absorption spectrum $\alpha_w(\omega)$ of liquid water [50].

The $P(\omega)$ power spectra, which represent the rate of scattering of energy by disperse systems, are

given in Fig. 8a. One or two characteristic peaks corresponding to the increase in dissipation of energy for both system I and systems IV–VII are observed in the initial part of the $P(\omega)$ spectrum, i.e., at $\omega < 1000$ cm^{-1}. In so doing, the maximal intensity of IR radiation for system I is higher than that for systems IV and V but lower than that for systems VI and VII. A significant increase in radiation power for systems binding atomic oxygen (VI and VII) is observed in the frequency range $\omega > 1000$ cm^{-1}. By and large, the increase in power P with frequency for pure disperse water occurs much faster than for disperse water systems holding molecular oxygen but much slower than for systems enriched with atomic oxygen. The highest rate of dissipation of energy stored by systems IV–VII is realized at frequencies of 2720, 3180, 3130, and 3350 cm^{-1}, respectively. The maximal values of power of radiation of systems I, IV–VII correlate as 1: 0.29: 0.13: 2.55: 1.79. Therefore, the dissociation of oxygen adsorbed by water clusters leads to a significant acceleration of dissipation of thermal energy, especially, in the frequency range $1000 \leqslant \omega \leqslant 3500$ cm^{-1}. Figure 8b shows the maximal power of IR radiation as a function of the number of water molecules in a cluster. One can see that the fastest dissipation of energy is characteristic of $(O)_2$ and $(O)_4(H_2O)_{35}$ clusters which hold atomic oxygen; in so doing, the power P for $(O)_2(H_2O)_{40}$ cluster is higher than that for $(O)_4(H_2O)_{35}$ aggregate.

4.3. Argon

The character of argon absorption by the $(H_2O)_{50}$ cluster is illustrated by Fig. 9, where the cluster configuration is shown 30 ps after the appearance of one (a) or two (b) atoms near the cluster. During this time, atoms came closer to the cluster so that they became its integral part. However, even in the case of the absorption of one atom, its penetration inside the cluster appeared to be hindered and, as a result, the atom was accommodated on the surface. The shape of a cluster changed due to the absorption of two atoms and its size along the line connecting atoms becomes shorter than the size in perpendicular direction. The solubility of argon in water is 2.37-fold higher than that of nitrogen [43]. In the case of dispersion medium, this difference is exhibited as the closer contact between atoms and water clusters than between N_2 molecules and the same cluster for the identical period of time.

The dielectric permittivity of aqueous disperse system changes substantially after the capture of argon atoms (Fig. 10). In this case, both the real and imaginary parts of ε increases appreciably at the frequencies $\omega > 1050$ cm^{-1} upon the absorption of one argon atom by each water cluster. The addition of the second argon atom to each water cluster decreases the ε' value throughout the studied frequency range. At the same time, the ε'' value decreases only at $\omega < 1670$ cm^{-1}; at the opposite sign of the inequality, the ε'' values of the dispersion medium that has captured two argon atoms per cluster are larger than frequency-correspondent ε'' value for pure dispersed water. At $\omega > 260$ cm^{-1}, the ε' values and, at $\omega > 680$ cm^{-1}, the ε'' value for all considered disperse systems becomes larger that corresponding characteristic for the bulk water [47,48].

The absorption of argon leads to a significant change in the absorption coefficient α of aqueous disperse system beginning with the frequency 1200 cm^{-1}, i.e., with the region, where intramolecular vibrations in water contribute mainly to the IR spectrum (Fig. 11). Note that a twofold increase in the concentration does not result in such strong changes in the $\alpha(\omega)$ spectrum as took place when passing from the pure dispersed water to the aqueous disperse system containing argon (system VIII). This also manifests that the change in the absorption spectrum is related with the changes in frequencies of intramolecular vibrations in water after the absorption of atoms by the clusters. The position of the major maximum of $\alpha(\omega)$ spectrum shifts from 3187 cm^{-1} for pure dispersed water (system I) to 3280 and 3390 cm^{-1}, respectively, for disperse systems VIII and IX that absorbed argon. In the region $\omega < 1200$ cm^{-1} of

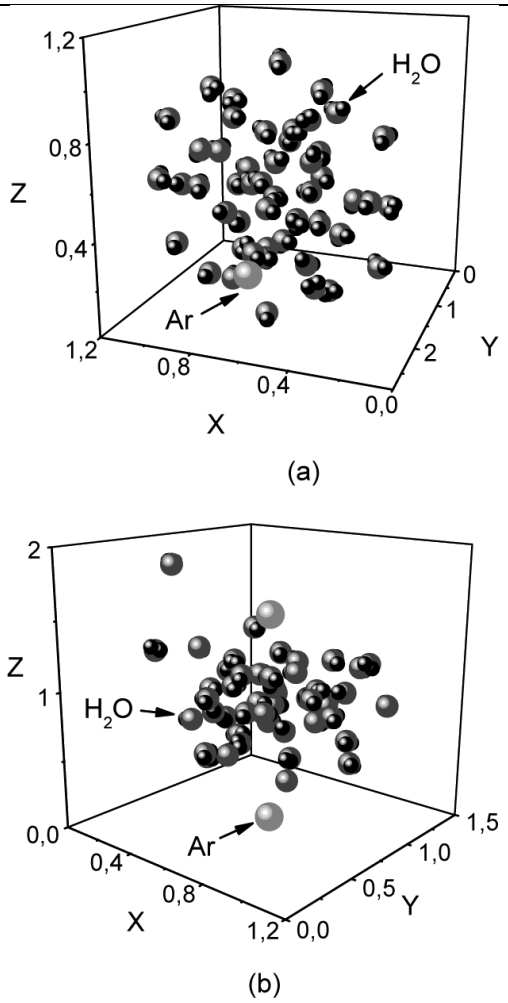

Fig. 9. Configurations of (a) $Ar(H_2O)_{50}$ and (b) $(Ar)_2(H_2O)_{50}$ clusters corresponding to time of 30 ps after the addition of Ar atoms to a system.

$\alpha(\omega)$ spectrum determined by vibrations of molecules, the major maximum also shifts toward higher frequencies (than 702 cm^{-1}, corresponding maximum of $\alpha(\omega)$ spectrum for pure dispersed water) after the absorption of atoms by the clusters.

Frequency dependences of P value for systems I, VIII, and IX are shown in Fig. 12a. It is seen that, as a result of the addition of one atom to each water cluster, the maximum emission power of IR radiation increases, at least, by the order of magnitude. However, the rate of energy dissipation drastically lowers due to the addition of one more atom to each cluster. Upon consecutive increase in the argon concentration, the position of the major maximum of $P(\omega)$ function shifts first to the left and then to the right so that, finally, these positions correspond to 3440, 3190, and 3400 cm^{-1} for systems I, VIII, and IX, respectively. The maximum of emission power as a function of the cluster size is shown in Fig. 12b. In system VIII, whose each cluster absorbs one atom, the $Ar(H_2O)_{40}$ aggregate demonstrates the highest rate of energy dissipation. The ability of this cluster to high-power emission is retained also after the absorption of one more atom.

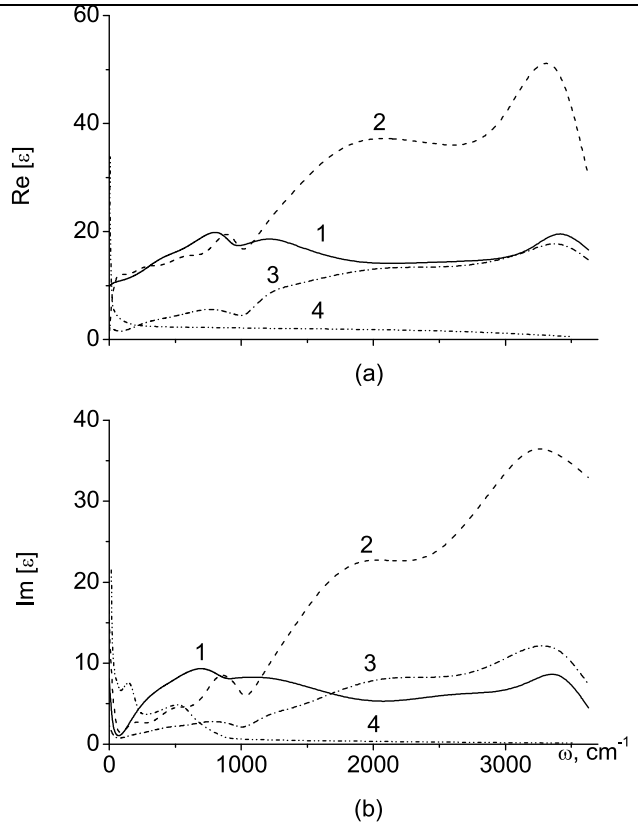

Fig. 10. (a) Real and (b) imaginary parts of the dielectric permittivity of disperse systems (1) I, (2), VIII, and (3) IX, and (4) bulk water. Panel (a): calculation, TIP4P model [48]. Panel (b): experiment [49].

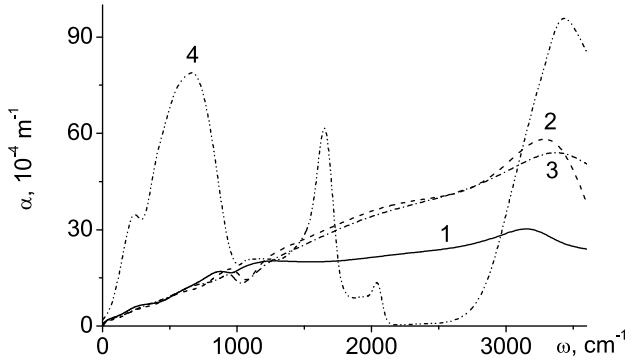

Fig. 11. Absorption coefficients of IR radiation of aqueous disperse systems (1) I, (2) VIII, and (3) IX, and (4) bulk water, experiment [50]. Curve 4 refers to the right-hand coordinate.

5. Summary and Conclusion

In this work we studied the absorption of nitrogen, oxygen, and argon by water clusters. The behavior of impurity in aqueous aggregates is strictly individual and is manifested in spectral characteristics. Hydrogen bonds, although much weaker than covalent bonds, still exert considerable influence on the

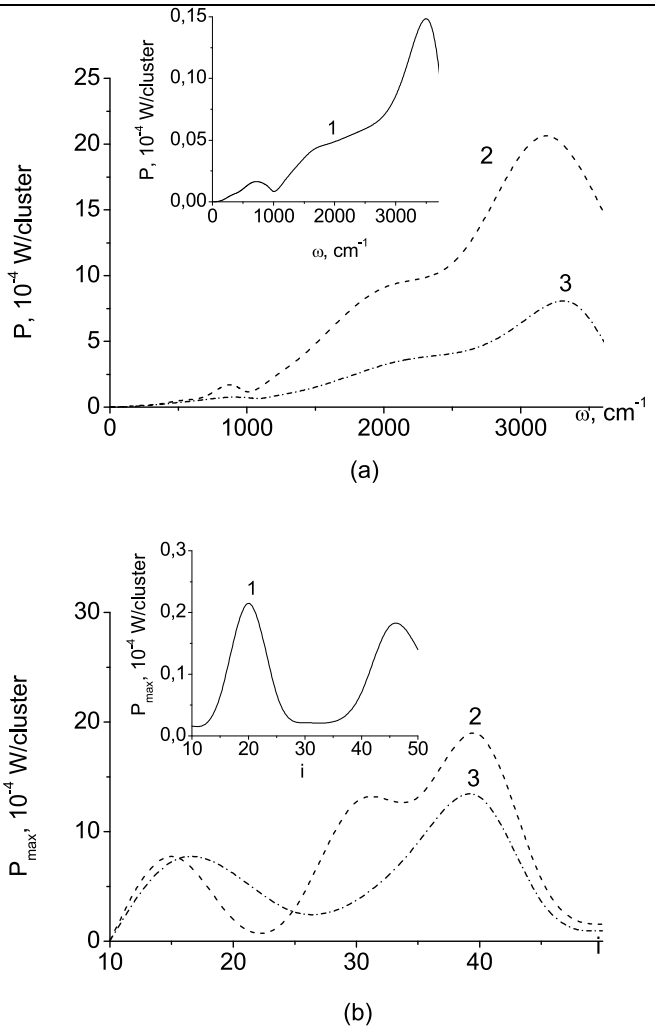

Fig. 12. (a) The power of radiation generated upon the dissipation of thermal energy; (b): maximum power of IR radiation in the ensembles of clusters containing i water molecules in different systems: (1) I, (2) VIII, and (3) IX.

properties of water clusters. The fundamental stretching frequency ($\sim$ 3400 cm^{-1}) of the O – H bond in water is particularly affected by the number of hydrogen bonds. Impurity as well as thermal agitation cause breaking and reforming of hydrogen bonds and change the IR spectrum. It is thought that oxygen "binds" water molecules, thus preventing cluster destruction and in turn eliminating the intensity enhancement of the dipole vibrations due to hydrogen bonding. It results in reduction of dielectric permittivity, especially its imaginary part. The adsorption of oxygen by disperse water systems leads to a decay of the absorption of IR radiation by these systems. Absorption of molecular and atomic oxygen renders various influences on spectral characteristics of disperse water systems. As the molecular oxygen concentration increases, the coefficient α of disperse water system decreases; when the atomic oxygen concentration increases at certain frequencies (for example, in the frequency range $1140 \leqslant \omega \leqslant 2880$ cm^{-1}), the value of α_V exceeds the values of α_{IV}. The capture of molecular oxygen by a disperse water system resulted in a significant decrease in the rate of dissipation P of the energy accumulated by

clusters; the absorption of atomic oxygen, on the contrary, was accompanied by a significant increase in P.

Due to "soft" repulsion, argon atoms are brought into closer contact with water molecules than nitrogen molecules for which the repulsion branch characterizing N-O interaction has a steeper form. This allows atoms to deeper penetrate into the water cluster, as compared with nitrogen molecules. The capture of one atom by each cluster results in a considerable increase in the real and imaginary parts of dielectric permittivity of system VIII composed of these species at frequency $\omega > 1050$ cm^{-1}. Such a behavior of $\varepsilon'(\omega)$ and $\varepsilon''(\omega)$ functions is not observed upon the capture of two atoms or the absorption of N_2 molecules by each cluster. The character of $\varepsilon'(\omega)$ and $\varepsilon''(\omega)$ dependences for system IX (when two Ar atoms are present in each cluster) is mainly similar to the behavior of these functions for the system composed of $(N_2)_2(H_2O)_i$ clusters, except for the facts that $\varepsilon'(\omega)$ function of system IX never intersects the plot of corresponding function for pure dispersed water and the $\varepsilon''(\omega)$ function of system IX somewhat earlier (beginning with frequency 1660 cm^{-1}) than system III acquires the values larger than $\varepsilon''(\omega)$ function of system I. The intersection point of the plots of $\varepsilon''(\omega)$ function for $(N_2)_2(H_2O)_i$ system and pure dispersed water corresponds to the frequency 1680 cm^{-1}, and the $\varepsilon'(\omega)$ function for system III reaches the value of analogous dependence for system I at the frequency 3100 cm^{-1}.

The absorption coefficients of IR radiation for systems I-III are similar at $\omega < 1000$ cm^{-1}. However, at $\omega > 1300$ cm^{-1}, the $\alpha(\omega)$ functions of these systems are divergent. Moreover, in this frequency range, system II has the largest values of α, while system I has the lowest values. Argon atoms adsorbed by water clusters are situated either on the surface or near the cluster surface. Such a position of atoms considerably changes the spectra of atomic intramolecular vibrations in clusters. This leads to a significant increase in the intensity of IR absorption spectra in a frequency range determined by intramolecular vibrations. As the concentration of absorbing gases rises twofold, coefficient α markedly decreases in this frequency range in the case of nitrogen absorption and slightly decreases upon the absorption of argon. The argon atom more often collides with water molecules in the cluster than it is observed for the N_2 molecule. Atoms of hydrogen and oxygen in water molecules appeared to be more excited in the presence of argon atoms in clusters, as compared with the presence of N_2 molecules. Correspondingly, the power of radiation generated upon the dissipation of thermal energy by the clusters increases to a larger extent in the case, when the impurity is represented by argon, and to a lesser extent, when nitrogen molecules are present in clusters. Twofold increase in the impurity concentration in a system lowers the average rate of energy dissipation by 2.7 and 1.5 times in the presence of argon and nitrogen in a system, respectively. The size of clusters that are most active to the emission of photons also depends on the type of impurity. In the case of argon, the most powerful energy emission is observed for $Ar(H_2O)_{40}$ and $(Ar)_2(H_2O)_{40}$ aggregates; among nitrogen-containing clusters, for $N_2(H_2O)_{50}$ and $(N_2)_2(H_2O)_{20}$ aggregates.

Thus, the basic atmospheric gases are capable of interacting with disperse water mediums. Absorption of these gases introduces appreciable changes in emission spectra of atmospheric moisture.

Acknowledgments

This work was supported by the Russian Foundation for Basic Research, project no. 08-08-00136.

References

[1] K.Ya. Kondrat'ev and N.I. Moskalenko, *Klyuchevyeproblemy issledovaniya planet solnechnoi sistemy.* (*Parnikovyi effekt atmosfer planet*) (Key Problems of Investigation of Solar System Planets: Greenhouse Effect of Planet Atmospheres), VINITI, Moscow, 1983.

[2] R. Wu, S. Vaupel, P. Nachtigall et al., *J Phys Chem, A* **108** (2004), 3338.
[3] G.E. Snow and G.T. Javor, *Origins* **2** (1975), 59.
[4] E. Chibowski, L. Holysz, A. Szczes and M. Chibowski, *Water Sci Technol* **49** (2004), 169.
[5] S. Liu, Z. Bacic and J.W. Moskowitz, *J Chem Phys* **101** (1994), 8310.
[6] B.J. Anderson, J.W. Tester and B.L. Trout, *J Phys Chem B* **108** (2004), 18705.
[7] P. Varanasi, S. Chou and S.S. Penner, *J Quant Spectrosc Radiat Transfer* **8** (1968), 1537.
[8] E.V. Akhmatskaya, C.J. Apps, I.H. Hillier, A.J. Masters, N.E. Watt and J.C. Whitehead, *Chem Commun* (1997), 707.
[9] T. Loerting and K.R. Liedl, *Proc Natl Acad Sci USA* **97** (2000), 8874.
[10] E.R. Lovejoy, D.R. Hanson and L.G. Huey, *J Phys Chem* **100** (1996), 19911.
[11] J.T. Jayne, U. Poschl, Y.M. Chen, D. Dai, L.T. Molina, D.R. Worsnop, C.E. Kolb and M.J. Molina, *J Phys Chem A* **101** (1997), 10000.
[12] Z. Slanina and J.F. Crifo, *Int J Thermophysics* **13** (1992), 465.
[13] S. Aloisio and J.S. Francisco, *J Phys Chem A* **102** (1998), 1899.
[14] S. Aloisio, J.S. Francisco and R.R. Friedl, *J Phys Chem A* **104** (2000), 6597.
[15] M. Kulmala, K.E.J. Lehtinen, L. Laakso, G. Mordas and K. Hämery, *Boreal Env Res* **10** (2005), 79.
[16] N. Goldman, R.S. Fellers, C. Leforestier and R.J. Saykally, *J Phys Chem* **105** (2001), 515.
[17] R.S. Fellers, C. Leforestier, L.B. Braly, M.G. Brown and R.J. Saykally, *Science* **284** (1999), 945.
[18] A. Miranowicz, R. Tanas and S. Kielich, *Quantum Opt* **2** (1990), 253.
[19] R. Tanaś and S. Kielich, *Quantum Opt* **2** (1990), 23.
[20] J.B. Klauda and S.I. Sandier, *J Phys Chem B* **106** (2002), 5722.
[21] O.A. Novruzova, V.N. Chukanov and A.E. Galashev, *Colloid Journal* **68** (2006), 462.
[22] H.L. Lemberg and F.H. Stillinger, *J Chem Phys* **62** (1975), 1677.
[23] A. Rahman, F.H. Stillinger and H.L. Lemberg, *J Chem Phys* **63** (1975), 5223.
[24] H. Saint-Martin, B. Hess and H.J.C. Berendsen, *J Chem Phys* **120** (2004), 11133.
[25] O.A. Novruzova, V.N. Chukanov and A.E. Galashev, *Colloid Journal* **68** (2006), 131.
[26] L.X. Dang and T.-M. Chang, *J Chem Phys* **106** (1997), 8149.
[27] W.S. Benedict, N. Gailar and E.K. Plyler, *J Chem Phys* **24** (1956), 1139.
[28] E.P. van Klaveren, J.P.J. Michels, J.A. Schouten et al., *J Chem Phys* **114** (2001), 5745.
[29] S. Kielich, *Physica* **28** (1962), 511.
[30] M.A. Spackman, *J Chem Phys* **85** (1986), 6579.
[31] M.A. Spackman, *J Chem Phys* **85** (1986), 6587.
[32] B.J. Anderson, J.W. Tester and B.L. Trout, *J PhysChem B* **108** (2004), 18705.
[33] F.H. Ree, *Simple Molecular Systems at Very High Density*, Plenum, NY, 1989.
[34] *Spravochnik khimika* (Chemist's Handbook), B.P. Nikol'skii, ed., Khimiya, Leningrad, 1971, vol. 1.
[35] J.M. Haile, *Molecular Dynamics Simulation. Elementary Methods*, Wiley, New York, 1992.
[36] V.N. Koshlyakov, *Ukr Mat Zh* **26** (1974), 200.
[37] V.N. Koshlyakov, *Zadachi dinamiki tverdogo tela I prikladnoi teorii giroskopov* (Problems of Solid Body Dynamics and Applied Theory of Gyroscopes), Nauka, Moscow, 1985.
[38] R.J. Sonnenschein, *Comput Phys* **59** (1985), 347.
[39] L.X. Dang and B.C. Garrett, *J Chem Phys* **99** (1993), 2972.
[40] H.J.C. Berendsen, J.R. Grigera and T.P. Straatsma, *J Phys Chem* **91** (1987), 6269.
[41] L. Landau, E. Lifshitz and L. Pitaevski, *Electrodynamics of Continuous Media*, Pergamon, Oxford,1984.
[42] *Fizicheskaya entsiklopediya* (Physical Encyclopedia), A.M. Prokhorov, ed., Moscow: Sovetskaya Entsiklope diya, 1988, vol. 1.
[43] F. Bresme, *J Chem Phys* **115** (2001), 7564.
[44] M. Neumann, *J Chem Phys* **82** (1985), 5663.
[45] W.B. Bosma, L.E. Fried and S. Mukamel, *J Chem Phys* **98** (1993), 4413.
[46] S. Horikawa, H. Itoh, J. Tabata et al., *J Phys Chem B* **101** (1997), 6290.
[47] A.G. Stromberg and D.P. Semchenko, *Fizicheskaya khimiya* (Physical Chemistry), Moscow: Vysshaya Shkola, 1988.
[48] M. Neumann, *J Chem Phys* **85** (1986), 1567.
[49] C.A. Angell and V. Rodgers, *J Chem Phys* **80** (1984), 6245.
[50] PL. Goggin and C. Carr, in: *Water and Aqueous Solutions*, G.W. Neilson and J.E. Enderby, eds, Adam Hilger, Bristol, 1986, vol. 37, p. 149.
[51] J.H. van der Maas, *Basic Infrared Spectroscopy*, Pitman Press, London, 1969.
[52] A.Y. Galashev and O.R. Rakhmanova, *Phys Lett A* **372** (2008), 3694.
[53] A.Y. Galashev, O.R. Rakhmanova, O.A. Galasheva and A.N. Novruzov, *Phase Trans* **79** (2006), 911.